

Spontaneous Magnetization of the $O(3)$ Ferromagnet at Low Temperatures

Christoph P. Hofmann

Department of Physics, University of California at San Diego, 9500 Gilman Drive, La Jolla, California 92093

(June 2001)

Abstract

We investigate the low-temperature behavior of ferromagnets with a spontaneously broken symmetry $O(3) \rightarrow O(2)$. The analysis is performed within the perspective of nonrelativistic effective Lagrangians, where the dynamics of the system is formulated in terms of Goldstone bosons. Unlike in a Lorentz-invariant framework (chiral perturbation theory), where loop graphs are suppressed by two powers of momentum, loops involving ferromagnetic spin waves are suppressed by three momentum powers. The leading coefficients of the low-temperature expansion for the partition function are calculated up to order p^{10} . In agreement with Dyson's pioneering microscopic analysis of the cubic ferromagnet, we find that, in the spontaneous magnetization, the magnon-magnon interaction starts manifesting itself only at order T^4 . The striking difference with respect to the low-temperature properties of the $O(3)$ antiferromagnet is discussed from a unified point of view, relying on the effective Lagrangian technique.

arXiv:cond-mat/0106492v1 24 Jun 2001

I. INTRODUCTION

In the following presentation, our interest is devoted to the low-temperature behavior of ferromagnets, which exhibit a spontaneously broken internal symmetry $O(3) \rightarrow O(2)$. This system has been widely studied in condensed matter physics and it is not our intention to contribute to its detailed microscopic understanding. Rather, we want to analyze several low-energy phenomena from a unified point of view, relying on the method of nonrelativistic effective Lagrangians. We try to understand how the symmetries, inherent in the underlying theory, manifest themselves in the partition function at low temperatures. The complex microscopic description of the system is taken into account only through a phenomenological parametrization, which, in the effective Lagrangian, emerges in the form of a few coupling constants.

Nevertheless, let us first consider the Heisenberg model, which describes the ferromagnet on a *microscopic* level. There, the exchange Hamiltonian \mathcal{H}_0 ,

$$\mathcal{H}_0 = -J \sum_{n.n.} \vec{S}_m \cdot \vec{S}_n, \quad J = \text{const}, \quad (1.1)$$

formulates the dynamics in terms of spin operators \vec{S}_m , attached to lattice sites m . Note that the summation only extends over nearest neighbors and that the isotropic interaction is assumed to be identical for any two adjacent lattice sites. For positive values of the exchange integral J , the above expression leads to an adequate low-energy description of the ferromagnet.

The interaction between a constant magnetic field $\vec{H} = (0, 0, H)$, $H > 0$, and the spin degrees of freedom is taken into account through the Zeeman term. In the corresponding extension of the Heisenberg model,¹

$$\mathcal{H} = \mathcal{H}_0 - \mu \sum_n \vec{S}_n \cdot \vec{H}, \quad (1.2)$$

the magnetic field is coupled to the vector of the total spin.

Within this model, Dyson evaluated the low-temperature expansion for the partition function of a ferromagnet for all three types of cubic lattices.² In particular, for the most prominent order parameter of the ferromagnet, the spontaneous magnetization, he obtained the following series:

$$\Sigma(T) / \Sigma(0) = 1 - \alpha_0 T^{\frac{3}{2}} - \alpha_1 T^{\frac{5}{2}} - \alpha_2 T^{\frac{7}{2}} - \alpha_3 T^4 + \mathcal{O}(T^{\frac{9}{2}}). \quad (1.3)$$

The $T^{3/2}$ -term, referred to as Bloch's law, corresponds to free magnons. The next two terms involving the coefficients α_1 and α_2 are related to the shape of the dispersion curve – or the discreteness of the lattice – and describe free magnons as well. Remarkably, the spin-wave interaction starts manifesting itself only at order T^4 .

In order to obtain this result, Dyson had to set up a highly involved mathematical machinery. It is our goal to rederive this series within the effective Lagrangian framework and to understand Dyson's result by exclusively considering the symmetries of the theory. In order to do so, we will first have to establish the momentum power counting scheme for this nonrelativistic system, which represents the very basis for a systematic expansion of

quantities of physical interest. As we will see, it is quite different from the power counting scheme in Lorentz-invariant effective theories (chiral perturbation theory).

Another aspect of the present work concerns the comparison of the low-energy properties of $O(3)$ ferromagnets and $O(3)$ antiferromagnets. Within the framework of nonrelativistic effective Lagrangians, we will, e.g., be able to understand the striking differences in the low-temperature expansions for the order parameters: the spontaneous magnetization for a ferromagnet and the staggered magnetization for an antiferromagnet, respectively.

In the effective Lagrangian perspective, the excitations near the ground state, the spin waves or magnons in the present case, are interpreted as Goldstone bosons resulting from a spontaneously broken internal symmetry. Indeed, the Heisenberg Hamiltonian (1.1) is invariant under a simultaneous rotation of the spin variables described by the symmetry group $G = O(3)$, whereas the ground state of a ferromagnet breaks this symmetry spontaneously down to $H = O(2)$: all the spins are aligned in one specific direction, giving rise to a nonzero spontaneous magnetization.

Whenever a physical system exhibits spontaneous symmetry breaking and the corresponding Goldstone bosons represent the only low-energy excitations without energy gap, we do have a very powerful means at our disposal to analyze its low-energy structure: effective Lagrangians. The method was originally developed in connection with Lorentz-invariant field theories (chiral perturbation theory),³⁻⁷ admitting a low-energy analysis of the strong interaction described by quantum chromodynamics (QCD). The effective Lagrangian technique has also proven to be very useful in the investigation of other relativistic systems where Goldstone bosons occur, see, e.g., Refs.⁸⁻¹⁰. The method has been extended to finite temperature,¹¹ allowing for a systematic low-temperature analysis of the partition function.

In condensed matter physics, spontaneous symmetry breaking is a common phenomenon and effective field theory methods are widely used in this domain. Only recently, however, has chiral perturbation theory been extended to such nonrelativistic systems,¹²⁻¹⁴ demonstrating its applicability to solid state physics as well. The method is based on effective Lagrangians which exploit the symmetry properties of the underlying theory, i.e., the Heisenberg model in the present case, and permits a systematic low-energy expansion of quantities of physical interest in powers of inverse wavelength. The few applications related to systems exhibiting collective magnetic behavior that appeared in the literature so far concern spin-wave scattering processes,¹⁵ spin-wave mediated non-reciprocal effects in antiferromagnets,¹⁶ the low-temperature expansion of the staggered magnetization of $O(N)$ antiferromagnets¹⁷ and spin waves in canted phases.¹⁴ An interesting application concerning $SO(5)$ invariance and high- T_c superconductivity can be found in Ref.¹⁸. Pedagogical introductions to effective Lagrangians are Refs.¹⁹⁻²¹, brief outlines of the method can be found in Refs.²².

As the effective analysis refers to large wavelengths, it does not resolve the microscopic structure of a solid and the system hence appears homogeneous. Accordingly, the effective Lagrangian is invariant with respect to translations. On the other hand, the effective Lagrangian is not invariant under rotations, since the lattice structure of a solid singles out preferred directions. In the case of a cubic lattice, the anisotropy, however, only shows up at higher orders of the derivative expansion:^{10,13} the discrete symmetries of a cubic lattice thus imply space rotation symmetry. In the following, we assume that the ferromagnet exhibits this type of lattice structure: the leading order effective Lagrangian is then invariant both under translations and under rotations and the corresponding expression for a ferromagnet

takes the form^{12,13}

$$\mathcal{L}_{eff}^2 = \Sigma \frac{\varepsilon_{ab} \partial_0 U^a U^b}{1 + U^3} + \Sigma \mu H U^3 - \frac{1}{2} F^2 \partial_r U^i \partial_r U^i. \quad (1.4)$$

In the above notation, the two real components of the magnon field, $U^a (a = 1, 2)$, have been collected in a three-dimensional unit vector $U^i = (U^a, U^3)$, which transforms with the vector representation of the rotation group $O(3)$. At leading order, the ferromagnet is thus characterized by two different low energy constants, Σ and F . The first term, which involves a time derivative, is related to a topological invariant. Remarkably, due to this contribution proportional to the spontaneous magnetization Σ , the effective Lagrangian of a ferromagnet fails to be invariant under the group $G = O(3)$. Note that such expressions, involving order parameters associated with the generators of the spontaneously broken group, would not be permitted in Lorentz-invariant effective theories. It represents the main novelty occurring in condensed matter physics, where nonrelativistic kinematics is less restrictive than Lorentz invariance.

The associated equation of motion is the Landau-Lifshitz equation,

$$\partial_0 U^a + \varepsilon_{ajk} f_0^j U^k + \gamma \varepsilon_{ajk} \Delta U^j U^k = 0, \quad f_0^j = \mu H \delta_3^j, \quad \gamma \equiv \frac{F^2}{\Sigma}, \quad (1.5)$$

which describes the dynamics of ferromagnetic spin waves. Its structure is of the Schrödinger type: first order in time, but second order in space. Note that, according to Goldstone's theorem, there have to be two real Goldstone fields in the case of a spontaneously broken symmetry $O(3) \rightarrow O(2)$. However, in the nonrelativistic regime, this does not necessarily imply that there also have to exist two independent magnon states. Indeed, in the present case of a ferromagnet, a complex field is required to describe one particle: there exists only *one* type of spin-wave excitation in a $O(3)$ ferromagnet, following a quadratic dispersion relation,

$$\omega(\vec{k}) = \gamma \vec{k}^2 + \mathcal{O}(|\vec{k}|^4). \quad (1.6)$$

Accordingly, in the effective description of this nonrelativistic system, **two** powers of momentum correspond to only **one** power of energy or temperature: $k^2 \propto \omega, T$.

The effective Lagrangian method provides us with a simultaneous expansion in powers of momentum and of the external field H . The important point is that, to a given order in the low-energy expansion, only a finite number of coupling constants and a finite number of graphs contribute. Let us now set up the effective Lagrangian for a ferromagnet at higher orders in the momentum expansion²³ and consider the corresponding power counting scheme.

II. POWER COUNTING AND EFFECTIVE LAGRANGIAN

In his pioneering microscopic analysis, Dyson evaluated the temperature expansion for the partition function of a cubic ferromagnet up to terms of order T^5 . In our effective language, where one power of temperature or energy counts like two powers of momentum, this corresponds to an expansion up to order p^{10} . We will now show that, to this order in the momenta, contributions to the effective Lagrangian involving at most six space derivatives

enter and the perturbative expansion requires the evaluation of graphs containing at most two loops.

First of all, note that there are no contributions to the effective Lagrangian with an odd number of space derivatives: parity excludes terms like

$$c_{abc} \varepsilon_{rst} \partial_r U^a \partial_s U^b \partial_t U^c, \quad (2.1)$$

which involve the antisymmetric tensor ε_{rst} .

Before constructing the relevant pieces $\mathcal{L}_{eff}^4, \mathcal{L}_{eff}^6, \dots$ step by step, we have to point out an important assumption underlying the present analysis: we assume that the effective Lagrangian of a ferromagnet is gauge invariant at subleading orders. In fact, the discrete symmetries of a cubic lattice and time-reversal invariance ensure that there is no topological contribution in \mathcal{L}_{eff}^4 (see Ref.¹³). Topological contributions which may show up in \mathcal{L}_{eff}^6 or beyond do not affect the conclusions of the present work.

Gauge invariance then implies that the magnetic field H enters the derivative expansion through a timelike covariant derivative,

$$D_0 U^i = \partial_0 U^i + \varepsilon_{ijk} f_0^j U^k, \quad f_0^j = \mu H \delta_3^j. \quad (2.2)$$

Note that the magnetic field occurs on the same level as the time derivative and is thus counted as a quantity of order p^2 .

The next-to-leading order Lagrangian is of order p^4 . It involves terms with two time derivatives, terms with one time and two space derivatives and terms with four space derivatives. Time derivatives, however, can be eliminated with the equation of motion,²⁴

$$\partial_0 U^a + \varepsilon_{ajk} f_0^j U^k + \gamma \varepsilon_{ajk} \Delta U^j U^k = 0,$$

such that we end up with the following independent terms:²⁵

$$\mathcal{L}_{eff}^4 = l_1 (\partial_r U^i \partial_r U^i)^2 + l_2 (\partial_r U^i \partial_s U^i)^2 + l_3 \Delta U^i \Delta U^i. \quad (2.3)$$

We thus have three effective coupling constants, l_1, l_2 and l_3 , at next-to-leading order. Note that all terms involving the magnetic field have been eliminated with the equation of motion. In particular, gauge invariance implies that there is no tree graph from \mathcal{L}_{eff}^4 contributing to the vacuum energy.

Clearly, the question now arises, to what order n in the effective Lagrangian \mathcal{L}_{eff}^{2n} we have to go to evaluate the partition function up to accuracy p^{10} . In the following, we will show that loop corrections involving ferromagnetic magnons are suppressed by *three* powers of momentum and the effective Lagrangian is needed up to \mathcal{L}_{eff}^6 .

To verify this statement, let us consider a scattering process. The effective Lagrangian provides us with an expansion for a multi-magnon scattering amplitude in powers of momentum. The elastic magnon-magnon scattering amplitude is obtained by expanding \mathcal{L}_{eff} up to order $(U^a U^a)^2$. As shown in Figure 1a, the leading term corresponds to the tree graph involving the four-magnon vertex from \mathcal{L}_{eff}^2 and is of order $F^2 \vec{k}^2 / \Sigma^2$ (see Ref.¹⁵). The first correction comes from the tree graph 1b with a vertex involving the next-to-leading order Lagrangian \mathcal{L}_{eff}^4 . However, we also have to consider loop graphs in the effective framework. These corrections are in general infinite and need to be renormalized.

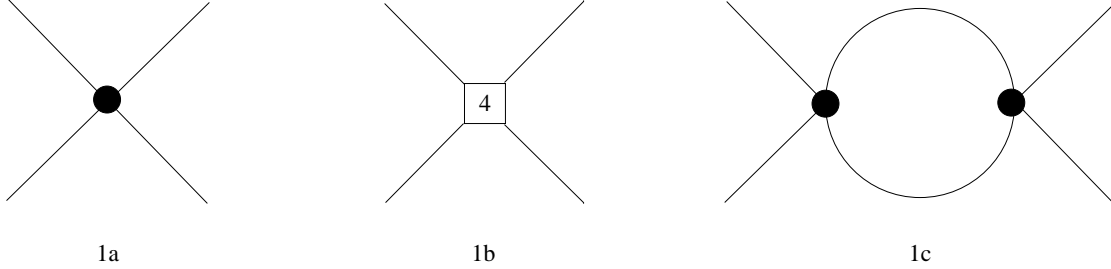


FIG. 1. Feynman graphs describing the leading contributions to the magnon-magnon scattering amplitude. The numbers attached to the vertices refer to the piece of the effective Lagrangian they come from. Vertices associated with the leading term \mathcal{L}_{eff}^2 are denoted by a dot.

Consider the magnon-magnon scattering graph 1c, where the two vertices come from \mathcal{L}_{eff}^2 . The form of the loop graph is

$$\mathcal{A}_{loop} \propto \int \frac{d\omega d^3k}{(2\pi)^4} \left(\frac{F^2 \vec{k}^2}{\Sigma^2} \right)^2 \left\{ \frac{1}{\omega - \gamma \vec{k}^2} \right\}^2, \quad (2.4)$$

where the quantities ω and \vec{k} denote generic energy and three momentum, respectively. Each four-magnon vertex from \mathcal{L}_{eff}^2 is of order $F^2 \vec{k}^2 / \Sigma^2$, while the two magnon propagators are of order $1/(\omega - \gamma \vec{k}^2)$. By dimensional analysis, the loop integral must then have the form

$$\mathcal{A}_{loop} \propto \frac{\gamma}{\Sigma^2} |\vec{p}|^5. \quad (2.5)$$

Comparing this expression with the leading tree graph amplitude 1a,

$$\mathcal{A}_{tree} \propto \frac{\gamma}{\Sigma} \vec{p}^2, \quad (2.6)$$

we find the remarkable result that, in the effective description of the ferromagnet, loops are suppressed by **three** powers of momentum. This is to be contrasted with the Lorentz-invariant framework (chiral perturbation theory), where loops are suppressed by two powers of momentum in four dimensions.

Hence, in order to carry out the expansion for the partition function up to accuracy p^{10} , we need the Lagrangian up to terms of order p^6 : \mathcal{L}_{eff}^6 shows up in a one-loop graph at order p^9 . Notice that the only relevant term coming from \mathcal{L}_{eff}^6 is quadratic in the magnon field. Eliminating time derivatives, we end up with

$$\mathcal{L}_{eff}^6 = c_1 U^i \Delta^3 U^i. \quad (2.7)$$

As in \mathcal{L}_{eff}^4 , terms involving the magnetic field do not show up: they have all been eliminated with the equation of motion. More generally, assuming $\mathcal{L}_{eff}^4, \mathcal{L}_{eff}^6, \mathcal{L}_{eff}^8$ and \mathcal{L}_{eff}^{10} to be gauge invariant, there are no tree-graph contributions from these higher order pieces of the effective Lagrangian to the vacuum energy – provided that the magnetic field is the only external field considered.

III. FINITE TEMPERATURE

In finite temperature field theory, the partition function is represented as a Euclidean functional integral,^{26–28}

$$\text{Tr}[\exp(-\mathcal{H}/T)] = \int [dU] \exp\left(-\int_{\mathcal{T}} d^4x \mathcal{L}_{eff}\right). \quad (3.1)$$

The integration is performed over all field configurations which are periodic in the Euclidean time direction $U(\vec{x}, x_4 + \beta) = U(\vec{x}, x_4)$, with $\beta \equiv 1/T$. The low-temperature expansion of the partition function is obtained by considering the fluctuations of the field U around the ground state $V = (0, 0, 1)$, i.e., by expanding U^3 in powers of U^a , $U^3 = \sqrt{1 - U^a U^a}$. The leading contribution is of order p^2 and contains a term quadratic in U^a which describes free magnons. In the presence of a magnetic field, they obey the dispersion relation²⁹

$$ik_4(\vec{k}) = \gamma \vec{k}^2 + \mu H + \mathcal{O}(|\vec{k}|^4). \quad (3.2)$$

The remainder of the effective Lagrangian is treated as a perturbation. Evaluating the Gaussian integrals in the standard manner, one arrives at a set of Feynman rules which differ from the conventional rules of the effective Lagrangian method only in one respect: the periodicity condition imposed on the Goldstone field modifies the propagator. At finite temperature, the propagator is given by

$$G(x) = \sum_{n=-\infty}^{\infty} \Delta(\vec{x}, x_4 + n\beta), \quad (3.3)$$

where $\Delta(x)$ is the Euclidean propagator at zero temperature,

$$\Delta(x) = \int \frac{dk_4 d^3k}{(2\pi)^4} \frac{e^{i\vec{k}\vec{x} - ik_4 x_4}}{\gamma \vec{k}^2 - ik_4 + \mu H}. \quad (3.4)$$

Note that the above Green function corresponds to the propagation of a single magnon, described by the complex field $u = U^1 + iU^2$.

We restrict ourselves to the infinite volume limit and evaluate the free energy density z , defined by

$$z = -T \lim_{L \rightarrow \infty} L^{-3} \ln [\text{Tr} \exp(-\mathcal{H}/T)]. \quad (3.5)$$

Temperature thus produces remarkably little change: to obtain the partition function, one simply restricts the manifold on which the fields are living to a torus \mathcal{T} in Euclidean space. The effective Lagrangian remains unaffected – the coupling constants F, Σ, l_1, \dots are temperature independent.

It is convenient to use dimensional regularization to evaluate the graphs of the effective theory. Unlike in a Lorentz-invariant framework, where the physical dimension d is equal to four, we regularize the nonrelativistic propagator only in the three spatial components,

$$\Delta(x) = \frac{1}{(2\pi)^d} \left(\frac{\pi}{\gamma}\right)^{\frac{d}{2}} \frac{1}{x_4^{\frac{d}{2}}} \exp\left(-\frac{\vec{x}^2}{4\gamma x_4} - \mu H x_4\right) \Theta(x_4), \quad (3.6)$$

and set $d = 3$ at the end of the calculation.

For the thermal propagator, we then have

$$G(x) = \frac{1}{(2\pi)^d} \left(\frac{\pi}{\gamma}\right)^{\frac{d}{2}} \sum_{n=-\infty}^{\infty} \frac{1}{x_n^{\frac{d}{2}}} \exp\left(-\frac{\vec{x}^2}{4\gamma x_n} - \mu H x_n\right) \Theta(x_n), \quad (3.7)$$

with

$$x_n \equiv x_4 + n\beta. \quad (3.8)$$

Using complex notation for the magnon field, the evaluation of Gaussian integrals simplifies, since the following two-point functions vanish:

$$\langle 0 | T \{ u(\vec{x}, x_4) u(\vec{y}, y_4) \} | 0 \rangle = \langle 0 | T \{ u^\dagger(\vec{x}, x_4) u^\dagger(\vec{y}, y_4) \} | 0 \rangle = 0. \quad (3.9)$$

Nonzero contributions to the partition function only result from

$$\langle 0 | T \{ u(\vec{x}, x_4) u^\dagger(\vec{y}, y_4) \} | 0 \rangle = \frac{2}{\Sigma} \Delta(x - y). \quad (3.10)$$

The calculation simplifies further due to space rotation symmetry of the propagator, implying that, at the origin, single space derivatives vanish,

$$\partial_r G(|\vec{x}|, x_4)|_{x=0} = 0. \quad (3.11)$$

Let us now evaluate the free energy density order by order in the momentum expansion.

IV. EVALUATION OF THE FREE ENERGY DENSITY

The relevant Feynman graphs are shown in Figure 2. Depicted are all contributions to the free energy density up to order p^{10} or, equivalently, order T^5 .

As we will see, all these contributions to the free energy density exclusively involve propagators, and space derivatives thereof, to be evaluated at the *origin* $x=0$. It is convenient to introduce the following notation:

$$\begin{aligned} G_1 &\equiv [G(x)]_{x=0}, \\ G_\Delta &\equiv [\Delta G(x)]_{x=0}, \end{aligned} \quad (4.1)$$

where Δ represents the Laplace operator in three dimensions – no confusion should occur with $\Delta(x)$, denoting the zero-temperature propagator.

The quantity G_1 is split into a finite piece, which is temperature dependent, and a divergent piece, which is temperature independent,

$$G_1 = G_1^T + G_1^0. \quad (4.2)$$

Using dimensional regularization, the explicit expressions are

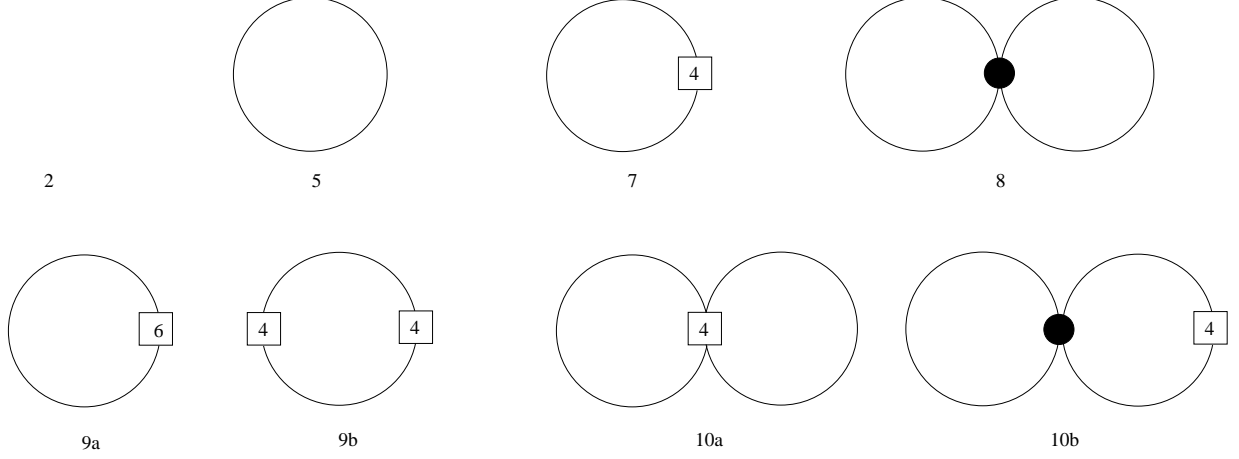


FIG. 2. Feynman graphs occurring in the low-temperature expansion of the partition function for an O(3) ferromagnet up to order p^{10} . The numbers attached to the vertices refer to the piece of the effective Lagrangian they come from. Vertices associated with the leading term \mathcal{L}_{eff}^2 are denoted by a dot. The numbers specifying individual graphs correspond to the power of momentum in the derivative expansion. Note that, in the counting scheme for ferromagnetic magnons, two powers of momentum correspond to one power of energy or temperature.

$$\begin{aligned}
 G_1^T &= \frac{1}{(2\pi)^d} \left(\frac{\pi}{\gamma}\right)^{\frac{d}{2}} \sum_{n=1}^{\infty} \frac{e^{-\mu H n \beta}}{(n\beta)^{\frac{d}{2}}}, \\
 G_1^0 &= \frac{1}{(2\pi)^d} \left(\frac{\pi}{\gamma}\right)^{\frac{d}{2}} \left[\frac{1}{x_4^{\frac{d}{2}}} \exp\left(-\frac{\vec{x}^2}{4\gamma x_4}\right) \Theta(x_4) \right]_{x=0}.
 \end{aligned} \tag{4.3}$$

Likewise, for G_{Δ} we have

$$\begin{aligned}
 G_{\Delta}^T &= \frac{1}{(2\pi)^d} \left(\frac{\pi}{\gamma}\right)^{\frac{d}{2}} \left(-\frac{d}{2\gamma}\right) \sum_{n=1}^{\infty} \frac{e^{-\mu H n \beta}}{(n\beta)^{\frac{d}{2}+1}}, \\
 G_{\Delta}^0 &= \frac{1}{(2\pi)^d} \left(\frac{\pi}{\gamma}\right)^{\frac{d}{2}} \left[\frac{1}{x_4^{\frac{d}{2}+1}} \left\{ \frac{-d}{2\gamma} + \frac{\vec{x}^2}{4\gamma^2 x_4} \right\} \exp\left(-\frac{\vec{x}^2}{4\gamma x_4}\right) \Theta(x_4) \right]_{x=0}.
 \end{aligned} \tag{4.4}$$

The temperature-independent pieces G_1^0 and G_{Δ}^0 , as well as propagators involving higher orders of space derivatives, are all related to momentum integrals of the form

$$\int d^d k \left(\vec{k}^2\right)^m \exp\left[-\gamma x_4 \vec{k}^2 - x_4 \mu H\right], \quad m = 0, 1, 2, \dots, \tag{4.5}$$

which are proportional to

$$\frac{\exp[-x_4 \mu H]}{(\gamma x_4)^{m+\frac{d}{2}}} \Gamma\left(m + \frac{d}{2}\right). \tag{4.6}$$

In dimensional regularization, however, these expressions vanish altogether: G_1^0 , G_{Δ}^0 and propagators involving more Laplacians do not contribute in the limit $d \rightarrow 3$. Therefore, in the evaluation of the above graphs, only the temperature-dependent pieces $G_1^T, G_{\Delta}^T, \dots$ are relevant.

The first contribution to the free energy density, which is of order p^2 , comes from tree graph 2. It does not depend on temperature and is given by

$$z_2 = -\Sigma\mu H. \quad (4.7)$$

The order p^5 contribution from one-loop graph 5 is associated with a d -dimensional nonrelativistic free Bose gas. For the temperature-dependent part, we obtain

$$z_5^T = -\frac{1}{8\pi^{\frac{3}{2}}\gamma^{\frac{3}{2}}} T^{\frac{5}{2}} \sum_{n=1}^{\infty} \frac{e^{-\mu H n \beta}}{n^{\frac{5}{2}}}. \quad (4.8)$$

At order p^7 , the next-to-leading order Lagrangian \mathcal{L}_{eff}^4 comes into play. For one-loop graph 7, which involves a two-magnon vertex, we get

$$z_7 = -\frac{2l_3}{\Sigma} \left[\Delta^2 G(x) \right]_{x=0}, \quad (4.9)$$

yielding

$$z_7^T = -\frac{15l_3}{16\pi^{\frac{3}{2}}\Sigma\gamma^{\frac{7}{2}}} T^{\frac{7}{2}} \sum_{n=1}^{\infty} \frac{e^{-\mu H n \beta}}{n^{\frac{7}{2}}}. \quad (4.10)$$

The first two-loop graph appears at order p^8 . Remarkably, this contribution is proportional to single space derivatives of the propagator at the origin and thus vanishes,

$$z_8 \propto \left[\partial_r G(x) \right]_{x=0} \left[\partial_r G(x) \right]_{x=0} = 0. \quad (4.11)$$

At order p^9 , two one-loop graphs show up which involve \mathcal{L}_{eff}^4 and \mathcal{L}_{eff}^6 , respectively. For graph 9a, we get

$$z_{9a} = -\frac{2c_1}{\Sigma} \left[\Delta^3 G(x) \right]_{x=0}, \quad (4.12)$$

leading to the temperature-dependent contribution

$$z_{9a}^T = \frac{105c_1}{32\pi^{\frac{3}{2}}\Sigma\gamma^{\frac{9}{2}}} T^{\frac{9}{2}} \sum_{n=1}^{\infty} \frac{e^{-\mu H n \beta}}{n^{\frac{9}{2}}}. \quad (4.13)$$

Graph 9b is proportional to an integral over the torus \mathcal{T} which involves a product of two propagators,

$$z_{9b} = -\frac{2l_3^2}{\Sigma^2} \int_{\mathcal{T}} d^{d+1}x \Delta^2 G(x) \Delta^2 G(-x). \quad (4.14)$$

This expression, however, can be reduced to an x -independent term involving one propagator only. To verify this statement, consider the equation for the thermal propagator,

$$\left(\frac{\partial}{\partial x_4} - \gamma\Delta + \mu H \right) G(x) = \delta(x), \quad (4.15)$$

and take the derivative with respect to the magnetic field. The quantity $\partial G(x)/\partial(\mu H)$ may then be written as a convolution integral over the torus. At the origin, the expression reads

$$\left[\frac{\partial G(x)}{\partial(\mu H)} \right]_{x=0} = - \int_{\mathcal{T}} d^{d+1}y G(-y) G(y). \quad (4.16)$$

Inserting Laplace operators at intermediate steps, we obtain the more general result

$$\left[\Delta^{(m+n)} \frac{\partial G(x)}{\partial(\mu H)} \right]_{x=0} = - \int_{\mathcal{T}} d^{d+1}y \Delta^m G(-y) \Delta^n G(y), \quad (4.17)$$

such that (4.14) can be written as

$$z_{9b} = \frac{2l_3^2}{\Sigma^2} \left[\Delta^4 \frac{\partial G(x)}{\partial(\mu H)} \right]_{x=0}. \quad (4.18)$$

For the temperature-dependent part of graph 9b, we then get

$$z_{9b}^T = - \frac{945 l_3^2}{64\pi^{\frac{3}{2}} \Sigma^2 \gamma^{\frac{11}{2}}} T^{\frac{9}{2}} \sum_{n=1}^{\infty} \frac{e^{-\mu H n \beta}}{n^{\frac{9}{2}}}. \quad (4.19)$$

Finally, at order p^{10} , two-loop graphs with insertions from \mathcal{L}_{eff}^4 show up. Graph 10a contributes with

$$z_{10a} = - \frac{2}{3\Sigma^2} (8l_1 + 6l_2 + 5l_3) G_{\Delta} G_{\Delta} - \frac{2l_3}{\Sigma^2} G_1 \left[\Delta^2 G(-x) \right]_{x=0}. \quad (4.20)$$

The evaluation of graph 10b amounts to

$$z_{10b} = \frac{2l_3}{\Sigma^2} G_1 \left[\Delta^2 G(-x) \right]_{x=0}, \quad (4.21)$$

and cancels the second term in z_{10a} . For the temperature-dependent part of order p^{10} we thus end up with

$$z_{10} = - \frac{3(8l_1 + 6l_2 + 5l_3)}{128\pi^3 \Sigma^2 \gamma^5} T^5 \left\{ \sum_{n=1}^{\infty} \frac{e^{-\mu H n \beta}}{n^{\frac{5}{2}}} \right\}^2. \quad (4.22)$$

Collecting terms, the result for the free energy density up to order p^{10} becomes

$$\begin{aligned} z = & -\Sigma\mu H - \frac{1}{8\pi^{\frac{3}{2}} \gamma^{\frac{3}{2}}} T^{\frac{5}{2}} \sum_{n=1}^{\infty} \frac{e^{-\mu H n \beta}}{n^{\frac{5}{2}}} - \frac{15l_3}{16\pi^{\frac{3}{2}} \Sigma \gamma^{\frac{7}{2}}} T^{\frac{7}{2}} \sum_{n=1}^{\infty} \frac{e^{-\mu H n \beta}}{n^{\frac{7}{2}}} \\ & - \frac{105}{32\pi^{\frac{3}{2}} \Sigma \gamma^{\frac{9}{2}}} \left(\frac{9l_3^2}{2\gamma\Sigma} - c_1 \right) T^{\frac{9}{2}} \sum_{n=1}^{\infty} \frac{e^{-\mu H n \beta}}{n^{\frac{9}{2}}} \\ & - \frac{3(8l_1 + 6l_2 + 5l_3)}{128\pi^3 \Sigma^2 \gamma^5} T^5 \left\{ \sum_{n=1}^{\infty} \frac{e^{-\mu H n \beta}}{n^{\frac{5}{2}}} \right\}^2. \end{aligned} \quad (4.23)$$

The first term is temperature-independent and originates from tree graph 2. Contributions which involve half integer powers of the temperature – $T^{5/2}$, $T^{7/2}$ and $T^{9/2}$, respectively – arise from one-loop graphs and are all related to the free energy density of noninteracting magnons. Remarkably, there is only one term in the above series, the order T^5 contribution coming from two-loop graph 10a, which is due to the magnon-magnon interaction.

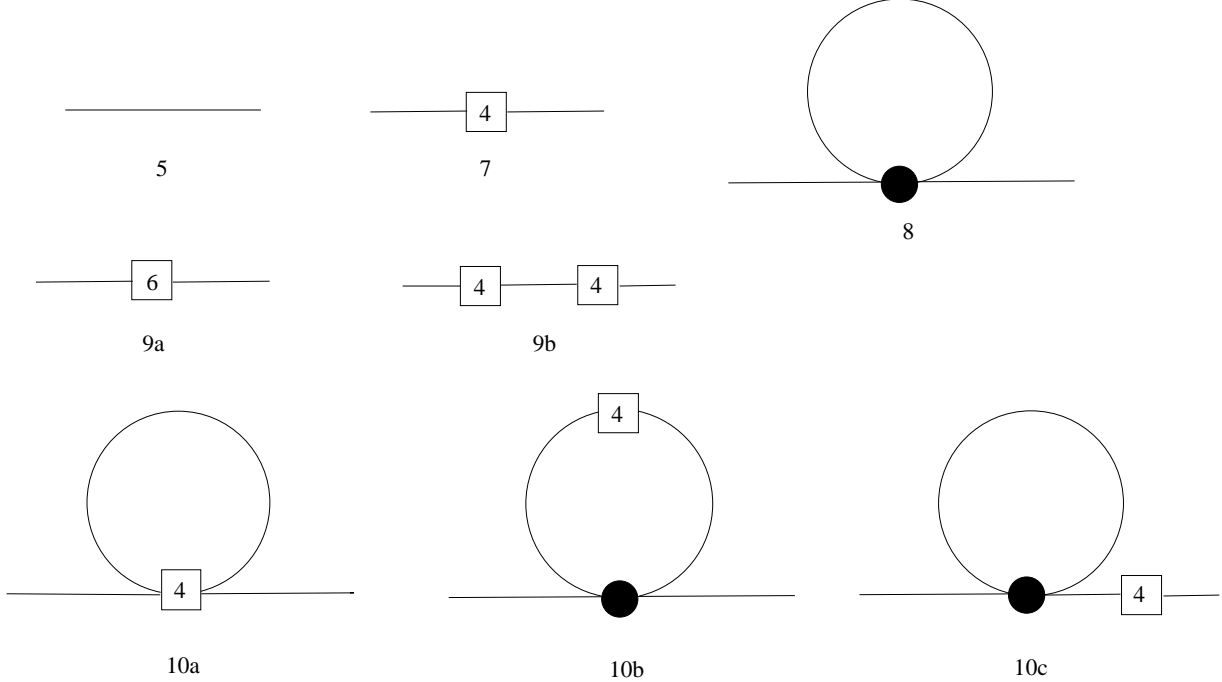


FIG. 3. Feynman graphs occurring in the low-energy expansion of the two-point function for an O(3) ferromagnet up to order p^{10} . The numbers specifying individual graphs correspond to the power of momentum in the derivative expansion.

V. INTERLUDE: FREE MAGNONS VERSUS INTERACTING MAGNONS

Consider the formula for the free energy density of a gas of noninteracting bosons,

$$z = z_0 + \frac{T}{(2\pi)^3} \int d^3k \ln(1 - e^{-\omega(\vec{k})/T}), \quad (5.1)$$

where z_0 is the energy density of the vacuum. With the leading term of the dispersion relation,

$$\omega(\vec{k}) = \gamma \vec{k}^2 + \mu H + \mathcal{O}(|\vec{k}|^4), \quad \gamma \equiv \frac{F^2}{\Sigma},$$

we readily reproduce the dominant one-loop contribution $z_5^T \propto T^{5/2}$ in the free energy density of the O(3) ferromagnet.

In order to account for subleading terms in the dispersion relation, we have to evaluate higher order contributions to the two-point function $\langle 0 | T \{ u(\vec{x}, x_4) u^\dagger(\vec{y}, y_4) \} | 0 \rangle$ of the magnon field. The relevant graphs are shown in Figure 3. Depicted are all contributions up to order p^{10} . Instead of listing individual results for the two-point function, we give the final expression for the dispersion relation originating from these graphs:

$$\omega(\vec{k}) = \frac{1}{\Sigma} (F^2 \vec{k}^2 + \Sigma \mu H - 2l_3 \vec{k}^4 + 2c_1 \vec{k}^6). \quad (5.2)$$

The two new terms correspond to graph 7, graph 9a and graph 9b of Figure 3. Note that one-loop graph 8 does not contribute to the dispersion relation. The effect of the three remaining one-loop graphs of order p^{10} will be discussed in a moment.

Inserting the above dispersion relation into formula (5.1), we reproduce all contributions to the free energy density which are associated with one-loop graphs: graphs 5, 7, 9a and 9b of Figure 2. These contributions are all related to noninteracting magnons – the corresponding coefficients in the dispersion relation are independent of the temperature.

As far as the evaluation of the three one-loop graphs of order p^{10} (Figure 3) is concerned, the situation is the following: in the sum of these contributions, only one term remains. It originates from graph 10a and leads to an additional term in the dispersion relation

$$\propto \frac{(8l_1 + 6l_2 + 5l_3)}{\Sigma^2} G_{\Delta}^0 \vec{k}^2. \quad (5.3)$$

However, in dimensional regularization, the quantity G_{Δ}^0 , as we have seen, vanishes, such that the dispersion relation is not affected by the graphs of order p^{10} .

Nevertheless, we can mimic the magnon-magnon interaction by allowing some of the coefficients of the dispersion relation to become temperature dependent. If we replace G_{Δ}^0 by G_{Δ}^T in (5.3), we obtain an interaction term proportional to T^5 in the free energy density. Moreover, we see that the leading order coupling constant γ is not renormalized at leading order ($\propto G_{\Delta}^T \vec{k}^2$, i.e., order p^8 in the free energy density), but only at next-to-leading order ($\propto G_{\Delta}^T \vec{k}^2$, i.e., order p^{10} in the free energy density). This observation, implying that the two-loop graph 8 does not contribute to the dispersion relation, was already made in Refs.³⁰.

In this section, we have split the free energy density into a piece corresponding to free magnons and a piece representing the magnon-magnon interaction,

$$z = z_{free} + z_{inter}. \quad (5.4)$$

The free part can be obtained from the free Bose gas formula

$$z_{free} = z_0 + \frac{T}{(2\pi)^3} \int d^3k \ln(1 - e^{-\omega(\vec{k})/T}),$$

with the modified dispersion relation

$$\omega(\vec{k}) = \frac{1}{\Sigma} \left\{ F^2 \vec{k}^2 + \Sigma \mu H - 2l_3 \vec{k}^4 + 2c_1 \vec{k}^6 \right\}.$$

The coupling constants F, Σ, l_3 and c_1 are all independent of the temperature. The interaction part originates from two-loop graph 10a which involves a four-magnon vertex from \mathcal{L}_{eff}^4 ,

$$z_{inter} = - \frac{3(8l_1 + 6l_2 + 5l_3)}{128\pi^3 \Sigma^2 \gamma^5} \left(\sum_{n=1}^{\infty} \frac{e^{-\mu H n \beta}}{n^{\frac{5}{2}}} \right)^2 T^5.$$

In order to make the structure of the low-temperature expansion for the free energy density of an O(3) ferromagnet more transparent, we rewrite the series in the form

$$z = z_0 - h_0 T^{\frac{5}{2}} - h_1 T^{\frac{7}{2}} - h_2 T^{\frac{9}{2}} - h_3 T^5 + \mathcal{O}(T^{\frac{11}{2}}), \quad (5.5)$$

where the temperature-dependent coefficients h_i are given by

$$\begin{aligned}
z_0 &= -\Sigma\mu H, \\
h_0 &= \frac{1}{8\pi^{\frac{3}{2}}\gamma^{\frac{3}{2}}} \sum_{n=1}^{\infty} \frac{e^{-\mu H n\beta}}{n^{\frac{5}{2}}}, \\
h_1 &= \frac{15 l_3}{16\pi^{\frac{3}{2}}\Sigma\gamma^{\frac{7}{2}}} \sum_{n=1}^{\infty} \frac{e^{-\mu H n\beta}}{n^{\frac{7}{2}}}, \\
h_2 &= \frac{105}{32\pi^{\frac{3}{2}}\Sigma\gamma^{\frac{9}{2}}} \left(\frac{9l_3^2}{2\gamma\Sigma} - c_1 \right) \sum_{n=1}^{\infty} \frac{e^{-\mu H n\beta}}{n^{\frac{9}{2}}}, \\
h_3 &= \frac{3(8l_1 + 6l_2 + 5l_3)}{128\pi^3\Sigma^2\gamma^5} \left(\sum_{n=1}^{\infty} \frac{e^{-\mu H n\beta}}{n^{\frac{5}{2}}} \right)^2.
\end{aligned} \tag{5.6}$$

In the limit $(\mu H/T) \rightarrow 0$, these coefficients become temperature independent and the sums reduce to Riemann zeta functions,

$$\begin{aligned}
\tilde{h}_0 &= \frac{1}{8\pi^{\frac{3}{2}}\gamma^{\frac{3}{2}}} \zeta\left(\frac{5}{2}\right), \\
\tilde{h}_1 &= \frac{15 l_3}{16\pi^{\frac{3}{2}}\Sigma\gamma^{\frac{7}{2}}} \zeta\left(\frac{7}{2}\right), \\
\tilde{h}_2 &= \frac{105}{32\pi^{\frac{3}{2}}\Sigma\gamma^{\frac{9}{2}}} \left(\frac{9l_3^2}{2\gamma\Sigma} - c_1 \right) \zeta\left(\frac{9}{2}\right), \\
\tilde{h}_3 &= \frac{3(8l_1 + 6l_2 + 5l_3)}{128\pi^3\Sigma^2\gamma^5} \zeta^2\left(\frac{5}{2}\right).
\end{aligned} \tag{5.7}$$

VI. SPONTANEOUS MAGNETIZATION

With the above representation for the free energy density, the low-temperature series for some relevant thermodynamic quantities can readily be derived. Since the system is homogeneous, the pressure is given by the temperature dependent part of the free energy density,

$$P = z_0 - z, \tag{6.1}$$

and the low-temperature expansion amounts to

$$P = h_0 T^{\frac{5}{2}} + h_1 T^{\frac{7}{2}} + h_2 T^{\frac{9}{2}} + h_3 T^5 + \mathcal{O}(T^{\frac{11}{2}}), \tag{6.2}$$

with coefficients h_i given in (5.6).

The first contribution represents the free Bose gas term which originates from one-loop graph 5. Subsequent terms exhibiting half integer powers of the temperature are related to the shape of the dispersion curve and represent effects due to the discreteness of the cubic lattice. Remarkably, there is no T^4 term in this series: two-loop graph 8 does not contribute. In the low-temperature expansion for the pressure, the interaction among ferromagnetic spin waves only starts manifesting itself at order T^5 .

The corresponding expressions for the energy density u , for the entropy density s and for the heat capacity c_V are readily worked out from the thermodynamic relations

$$s = \frac{\partial P}{\partial T}, \quad u = Ts - P, \quad c_V = \frac{\partial u}{\partial T} = T \frac{\partial s}{\partial T}. \quad (6.3)$$

Reordering powers of the temperature and taking the limit $(\mu H/T) \rightarrow 0$, we get

$$\begin{aligned} u &= \frac{3}{2} \tilde{h}_0 T^{\frac{5}{2}} + \frac{5}{2} \tilde{h}_1 T^{\frac{7}{2}} + \frac{7}{2} \tilde{h}_2 T^{\frac{9}{2}} + 4\tilde{h}_3 T^5 + \mathcal{O}(T^{\frac{11}{2}}), \\ s &= \frac{5}{2} \tilde{h}_0 T^{\frac{3}{2}} + \frac{7}{2} \tilde{h}_1 T^{\frac{5}{2}} + \frac{9}{2} \tilde{h}_2 T^{\frac{7}{2}} + 5\tilde{h}_3 T^4 + \mathcal{O}(T^{\frac{9}{2}}), \\ c_V &= \frac{15}{4} \tilde{h}_0 T^{\frac{3}{2}} + \frac{35}{4} \tilde{h}_1 T^{\frac{5}{2}} + \frac{63}{4} \tilde{h}_2 T^{\frac{7}{2}} + 20\tilde{h}_3 T^4 + \mathcal{O}(T^{\frac{9}{2}}), \end{aligned} \quad (6.4)$$

with coefficients \tilde{h}_i given in (5.7).

Let us now consider the low-temperature expansion for the spontaneous magnetization,

$$\Sigma(T) = - \lim_{H \rightarrow 0} \frac{\partial z}{\partial(\mu H)}. \quad (6.5)$$

With the expression (5.5) for the free energy density, we obtain the following series:

$$\Sigma(T) / \Sigma = 1 - \alpha_0 T^{\frac{3}{2}} - \alpha_1 T^{\frac{5}{2}} - \alpha_2 T^{\frac{7}{2}} - \alpha_3 T^4 + \mathcal{O}(T^{\frac{9}{2}}). \quad (6.6)$$

The coefficients α_n are independent of the temperature and given by

$$\begin{aligned} \alpha_0 &= \frac{1}{8\pi^{\frac{3}{2}} \Sigma \gamma^{\frac{3}{2}}} \zeta\left(\frac{3}{2}\right), \\ \alpha_1 &= \frac{15 l_3}{16\pi^{\frac{3}{2}} \Sigma^2 \gamma^{\frac{7}{2}}} \zeta\left(\frac{5}{2}\right), \\ \alpha_2 &= \frac{105}{32\pi^{\frac{3}{2}} \Sigma^2 \gamma^{\frac{9}{2}}} \left(\frac{9l_3^2}{2\gamma \Sigma} - c_1 \right) \zeta\left(\frac{7}{2}\right), \\ \alpha_3 &= \frac{3(8l_1 + 6l_2 + 5l_3)}{64\pi^3 \Sigma^3 \gamma^5} \zeta\left(\frac{5}{2}\right) \zeta\left(\frac{3}{2}\right). \end{aligned} \quad (6.7)$$

Here comes the appropriate place where we would like to compare our result with Dyson's microscopic calculation. In fact, one of the main motivations for his analysis was the following question: at what order in the low-temperature expansion does the spin-wave interaction manifest itself in the spontaneous magnetization? Before his rigorous analysis, in which he showed that the spin-wave interaction only starts contributing at order T^4 , there appeared to be an amazing mess in the literature. At least three different answers were available, all of them in contradiction with each other and, as it turned out, also in contradiction with Dyson's result: the authors³¹ obtained a term proportional to T^2 and the two references^{32,33} ended up with two different contributions of order $T^{7/4}$.

Within the effective Lagrangian framework we clearly confirm Dyson's finding: in the spontaneous magnetization, the leading contribution coming from the magnon-magnon interaction is of order T^4 . Any microscopic information, such as the specification of the type of the cubic lattice, is comprised in the numerical values of the effective coefficients α_n – they involve the coupling constants F, Σ, l_1, \dots occurring in the derivative expansion of the effective Lagrangian $\mathcal{L}_{eff}^2, \mathcal{L}_{eff}^4$ and \mathcal{L}_{eff}^6 , which phenomenologically parametrize the microscopic detail.

After Dyson's work, various authors tried to derive his results with alternative methods within the microscopic framework of the Heisenberg model. In particular, there was emerging interest in simplifying his complicated calculation.³⁴ In the course of these investigations, however, not all authors could confirm Dyson's findings and, surprisingly, a new term in the temperature expansion for the spontaneous magnetization started to haunt the literature: various authors³⁵ ended up with an interaction term of order T^3 . However, the T^3 contribution turned out to be a spurious effect.³⁶ It emerged due to the approximation methods used in these involved microscopic calculations: random phase approximation and decoupling approximation in the method of double-time temperature-dependent Green functions.

We would like to emphasize that there are no such approximations in the effective Lagrangian framework. The method applies to any system where the Goldstone bosons are the only excitations without energy gap. In the effective Lagrangian perspective, the problem is approached from a unified and model-independent point of view, based on the symmetries inherent in the underlying theory. In the present case of a ferromagnet, it is the spontaneously broken internal symmetry $O(3) \rightarrow O(2)$ of the Heisenberg model and the nonzero value for the spontaneous magnetization, which dictate the structure of the low-temperature series considered in this paper.

Our calculation clearly shows that there is no T^3 term in the low-temperature expansion for the spontaneous magnetization of a cubic $O(3)$ ferromagnet. Using effective language this translates into the statement that the contribution from two-loop graph 8 of Figure 2 to the free energy density vanishes. As we have pointed out, the reason is due to space rotation symmetry of the leading order effective Lagrangian, implying that single space derivatives of the propagator, evaluated at the origin, are zero.

The argument is not restricted to cubic lattices. Consider the leading order Lagrangian of the $O(3)$ ferromagnet:

$$\mathcal{L}_{eff}^2 = \Sigma \frac{\varepsilon_{ab} \partial_0 U^a U^b}{1 + U^3} + \Sigma \mu H U^3 - \frac{1}{2} F^2 \partial_r U^i \partial_r U^i .$$

Let us replace the last term, which is invariant under space rotations, by the more general expression

$$- \frac{1}{2} F_1^2 \partial_1 U^i \partial_1 U^i - \frac{1}{2} F_2^2 \partial_2 U^i \partial_2 U^i - \frac{1}{2} F_3^2 \partial_3 U^i \partial_3 U^i , \quad (6.8)$$

in order to account for anisotropies of the crystal lattice. The modified equation for the thermal propagator,

$$\left(\frac{\partial}{\partial x_4} - \gamma_1 \partial_1^2 - \gamma_2 \partial_2^2 - \gamma_3 \partial_3^2 + \mu H \right) G(x) = \delta(x) , \quad (6.9)$$

again, allows us to eliminate all terms in the evaluation of graph 8 up to contributions which involve single space derivatives of the propagator at the origin,

$$z_8 = \sum_p c_p \left[\partial_p G(x) \right]_{x=0} \left[\partial_p G(x) \right]_{x=0} , \quad p = 1, 2, 3 . \quad (6.10)$$

Even though the thermal propagator is no longer space rotation symmetric, it is still invariant under parity, such that single space derivatives, evaluated at the origin, vanish. We conclude that, also for anisotropic lattices, described by the new contributions (6.8) in the effective Lagrangian, there is no interaction term of order T^3 in the low-temperature series for the spontaneous magnetization.

VII. ORDER PARAMETERS OF FERRO- AND ANTIFERROMAGNETS: SPONTANEOUS VERSUS STAGGERED MAGNETIZATION

The low-energy behavior of an O(3) ferromagnet is determined by the spin waves which represent the Goldstone bosons of this nonrelativistic system. These low-energy excitations obey a *quadratic* dispersion relation. As is well-known, the spin waves of an *antiferromagnet*, on the other hand, follow a *linear* dispersion law. Accordingly, the low-temperature properties of these two systems are quite different – the difference reveals itself, e.g., in the low-temperature expansion for the corresponding order parameters. In this section we are going to address the two systems within the effective Lagrangian perspective.

The low-temperature analysis of an O(N) antiferromagnet, exhibiting a spontaneously broken internal symmetry $O(N) \rightarrow O(N-1)$, was the object of reference.¹⁷ Here, we only want to point out some basic ingredients in order to compare the system with the ferromagnet.

In the underlying theory, the O(N) symmetry of the Heisenberg model is explicitly broken by an external anisotropy field \vec{h} . It is convenient to collect the (N–1) Goldstone fields U^a in a N-dimensional vector $U^i = (U^0, U^a)$ of unit length,

$$U^i(x) U^i(x) = 1, \quad (7.1)$$

and to take the constant external field along the zeroth axis, $h^i = (h, 0, \dots, 0)$. The Euclidean form of the effective Lagrangian for an O(N) antiferromagnet up to order p^4 then reads:⁸

$$\begin{aligned} \mathcal{L}_{eff}^{AF} = & \frac{1}{2} \mathcal{F}^2 \partial_\mu U^i \partial_\mu U^i - \Sigma_s h^i U^i - e_1 (\partial_\mu U^i \partial_\mu U^i)^2 - e_2 (\partial_\mu U^i \partial_\nu U^i)^2 \\ & + k_1 \frac{\Sigma_s}{\mathcal{F}^2} (h^i U^i) (\partial_\mu U^k \partial_\mu U^k) - k_2 \frac{\Sigma_s^2}{\mathcal{F}^4} (h^i U^i)^2 - k_3 \frac{\Sigma_s^2}{\mathcal{F}^4} h^i h^i. \end{aligned} \quad (7.2)$$

In the power counting scheme, the field $U(x)$ counts as a quantity of order one. For the antiferromagnet, derivatives correspond to one power of the momentum, $\partial_\mu \propto p$, whereas the external field h counts as a quantity of order p^2 . Hence, at leading order ($\propto p^2$) two coupling constants, \mathcal{F} and Σ_s , occur, at next-to-leading order ($\propto p^4$) we have five such constants, e_1, e_2, k_1, k_2, k_3 .

The essential point here is the fact that a term involving a single time derivative does not show up in the effective Lagrangian: this topological contribution is proportional to the spontaneous magnetization which, in the case of an antiferromagnet, vanishes. Hence, the corresponding equation of motion is of second order both in space and in time, its relativistic structure determining the number of independent magnon states: the Fourier decomposition contains both positive and negative frequencies, such that a single real field suffices to describe one particle. Accordingly, there exist *two* different types of spin-wave excitations in an antiferromagnet – as it is the case in Lorentz-invariant theories, Goldstone fields and Goldstone particles are in one-to-one correspondence. These low-energy excitations follow a linear dispersion relation. As a consequence, in the power counting scheme for antiferromagnetic magnons, powers of momentum are on the same footing as powers of energy or temperature: $k^2 \propto \omega^2, T^2$.

Let us now turn to the evaluation of the partition function of an O(N) antiferromagnet, $N \geq 2$. The relevant graphs are depicted in Figure 4. Lorentz invariance ensures that only

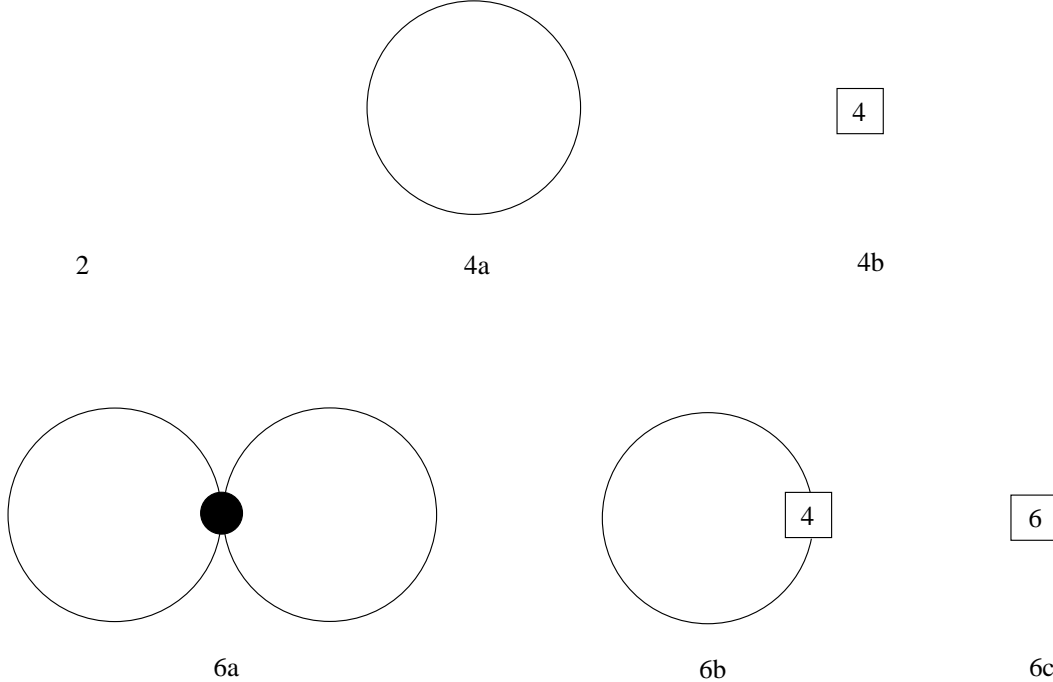


FIG. 4. Feynman graphs occurring in the low-temperature expansion for the partition function of an $O(N)$ antiferromagnet up to order p^6 . The numbers attached to the vertices refer to the piece of the effective Lagrangian they come from. Vertices associated with the leading term of \mathcal{L}_{eff}^{AF} are denoted by a dot. The numbers specifying individual graphs correspond to the power of momentum in the derivative expansion. Note that, in the counting scheme for antiferromagnetic magnons, two powers of momentum correspond to two powers of energy or temperature.

even powers of momentum occur and that loop graphs are suppressed by *two* powers of momentum. Shown are all contributions to the free energy density up to order p^6 or, equivalently, T^6 . Note the striking difference with respect to Figure 2, which displays the Feynman graphs relevant for the evaluation of the partition function of an $O(3)$ ferromagnet.

The tree graphs 4b and 6c are temperature independent and hence merely renormalize the vacuum energy. One-loop graph 6b exclusively contains a vertex which is quadratic in the Goldstone boson field and thus only contributes to a renormalization of the mass $M^2 = \Sigma_s h / \mathcal{F}^2$ in the free Bose gas term related to graph 4a. The final expression for the renormalized mass takes the form³⁷

$$M_\pi^2 = \frac{\Sigma_s h}{\mathcal{F}^2} + \frac{N-3}{32\pi^2} \frac{(\Sigma_s h)^2}{\mathcal{F}^6} \ln \frac{h}{h_M} + \mathcal{O}(h^3). \quad (7.3)$$

The logarithmic scale h_M is determined by k_1 and k_2 , i.e., by two next-to-leading order coupling constants (order p^4). The occurrence of such "chiral logarithms" is characteristic of the effective Lagrangian method in the Lorentz-invariant regime. To the order p^6 considered here, we are thus left with only one candidate for the interaction: two-loop graph 6a.

In the limit of a zero external field, the low-temperature expansion of the pressure amounts to

$$P^{AF} = \frac{1}{90} \pi^2 (N-1) T^4 + \mathcal{O}(T^8). \quad (7.4)$$

The T^4 contribution represents the free Bose gas term which originates from one-loop graph 4a. The effective interaction among the Goldstone bosons, remarkably, only manifests itself through a term of order T^8 , which is beyond the scope of the present discussion. As it turns out, the contribution of order p^6 coming from two-loop graph 6a, is proportional to the external field, such that, in the limit $h \rightarrow 0$ considered here, it vanishes.

It is interesting to note that this two-loop graph, which involves a four magnon-vertex from the leading Lagrangian \mathcal{L}_{eff}^2 , does not contribute to the pressure of an O(3) ferromagnet, either. The reason, however, is quite different. For the antiferromagnet, the contribution is only absent in zero external field, whereas for the ferromagnet the contribution from graph 8 vanishes because of space rotation symmetry or parity.

Let us now turn to the order parameters. In the case of an O(3) antiferromagnet this quantity is referred to as staggered magnetization. It is given by the logarithmic derivative of the partition function with respect to the external field h and, for an O(N) antiferromagnet, the low-temperature expansion amounts to (for details see¹⁷)

$$\Sigma_s(T) / \Sigma_s(0) = 1 - \frac{N-1}{24} \frac{T^2}{\mathcal{F}^2} - \frac{(N-1)(N-3)}{1152} \frac{T^4}{\mathcal{F}^4} + \mathcal{O}(T^6). \quad (7.5)$$

On the other hand, the low-temperature expansion for the spontaneous magnetization of the O(3) ferromagnet, derived in the present paper, reads

$$\Sigma(T) / \Sigma(0) = 1 - \alpha_0 T^{\frac{3}{2}} - \alpha_1 T^{\frac{5}{2}} - \alpha_2 T^{\frac{7}{2}} - \alpha_3 T^4 + \mathcal{O}(T^{\frac{9}{2}}).$$

Comparing these formulae for the staggered and spontaneous magnetization, respectively, the following issues are worth pointing out.

Obviously, as far as the structure of the low-temperature expansion is concerned, the two series are quite different. The leading terms ($\propto T^2$ for the antiferromagnet, $\propto T^{3/2}$ for the ferromagnet) are an immediate consequence of the corresponding dispersion laws: linear for the antiferromagnet, quadratic for the ferromagnet. They are both related to a one-loop graph.

Now we have to emphasize that the evaluation of the partition function for the antiferromagnet was performed in a Lorentz-invariant framework, exhibiting a relativistic dispersion law

$$\omega^2 = v^4 M^2 + v^2 \vec{k}^2, \quad (7.6)$$

with the speed of light replaced by the spin-wave velocity v . The point is that we did not consider corrections proportional to $\vec{k}^4, \vec{k}^6, \dots$ in the dispersion relation in order to account for the discreteness of the lattice. Equivalently, we did not consider terms in the subleading pieces $\mathcal{L}_{eff}^4, \mathcal{L}_{eff}^6, \dots$ of the effective Lagrangian which, although space rotation invariant, are no longer Lorentz invariant. They would have manifested themselves as terms of order T^4, T^6, \dots in the staggered magnetization of the antiferromagnet. Like the analogous terms of order $T^{5/2}, T^{7/2}, \dots$ in the spontaneous magnetization of the ferromagnet, these contributions merely correspond to noninteracting magnons.

What is remarkable, however, is the fact that the two-loop contribution involving a four-magnon vertex from the leading piece \mathcal{L}_{eff}^2 of the effective Lagrangian vanishes in either case: in the low-temperature series for the staggered and spontaneous magnetization, the

spin-wave interaction does not manifest itself through this graph. Note that the reasons are different. For an $O(N)$ antiferromagnet, there is actually a term proportional to T^4 in the low-temperature series (7.5) for the order parameter. But for the particular case $N=3$ we are considering, the term does not show up in the staggered magnetization – corrections associated with the magnon interaction only appear at order T^6 .¹⁷ On the other hand, the two-loop contribution for the ferromagnet, proportional to T^3 , vanishes due to space rotation symmetry – corrections originating from the magnon interaction manifest themselves through the Dyson term proportional to four powers of the temperature.

Another striking difference concerns the fact that for the antiferromagnet, the low-temperature expansion is completely fixed by a single coupling constant \mathcal{F} up to order T^4 , i.e., including the first correction coming from the interaction.³⁸ This is not the case for the ferromagnet, where the leading interaction term, i.e., the two-loop contribution $\alpha_3 T^4$, involves coupling constants from the next-to-leading order Lagrangian \mathcal{L}_{eff}^4 . We conclude that, for Lorentz-noninvariant systems, kinematics is much less restrictive – less information is available via symmetry considerations, such that more phenomenological input for the corresponding nonrelativistic system is required.

VIII. CONCLUSIONS AND OUTLOOK

The low-energy behavior of an $O(3)$ ferromagnet is determined by its low-energy excitations, the magnons or spin waves, which represent the Goldstone bosons of the spontaneously broken internal symmetry $O(3) \rightarrow O(2)$. The system may be analyzed within the framework of nonrelativistic effective Lagrangians, which tackles the phenomenon of spontaneous symmetry breaking from a unified point of view. The method exploits the symmetry properties of the underlying theory, i.e., the Heisenberg model in the present case, and formulates the dynamics in terms of Goldstone boson fields. At large wavelengths, the microscopic structure of condensed matter systems does not play a significant role: in the corresponding effective Lagrangian, the specific properties of the system only manifest themselves in the numerical values of a few coupling constants.

The low-energy excitations of an $O(3)$ ferromagnet obey a *quadratic* dispersion relation. In the momentum power counting scheme, which provides us with a systematic expansion of physical quantities in powers of inverse wavelength, two powers of momentum thus correspond to only one power of energy or temperature. Remarkably, unlike in a Lorentz-invariant framework where loop corrections are suppressed by two powers of momentum, loops involving ferromagnetic magnons are suppressed by three momentum powers.

In this nonrelativistic framework, the evaluation of the partition function for an $O(3)$ ferromagnet is presented up to order p^{10} : up to order T^5 in the free energy density or, equivalently, up to order T^4 in the spontaneous magnetization. In agreement with Dyson’s microscopic analysis, we find that, in the spontaneous magnetization, the spin-wave interaction only starts contributing at order T^4 . Moreover, within the effective Lagrangian perspective we readily understand the absence of a T^3 term in the spontaneous magnetization. This spurious term, which was the object of various microscopic investigations, vanishes because of space rotation symmetry or parity of the leading order effective Lagrangian. The effective Lagrangian method not only proves to be more efficient than the complicated microscopic

analysis, but also addresses the problem from a model-independent point of view based on the symmetries of the system.

It is very instructive to compare the $O(3)$ ferromagnet and the $O(3)$ antiferromagnet within the framework of effective Lagrangians. Spin waves in antiferromagnets obey a linear dispersion relation, implying that powers of momentum, energy and temperature are all on the same footing: the power counting is identical with the standard, Lorentz-invariant scheme. Accordingly, the low-temperature properties of these two systems are quite different as illustrated by the low-temperature expansion for the pressure and for the corresponding order parameters, the spontaneous and staggered magnetization, respectively.

Having established the power counting scheme for the ferromagnet, we have paved the way for further investigations of this nonrelativistic system within the effective Lagrangian perspective. In fact, the low-temperature expansion for the partition function has already been carried to order p^{11} , where the first three-loop graphs show up. An outline of the calculation, which goes beyond Dyson's microscopic analysis, will be presented in a forthcoming paper.³⁹

ACKNOWLEDGMENTS

It is a pleasure to thank H. Leutwyler for numerous stimulating discussions and for his patient assistance throughout this work. Thanks also to S. Mallik, A.V. Manohar, D. Toublan and J. Soto for their help. I am greatly indebted to the Holderbank-Stiftung for support. Likewise, support by Schweizerischer Nationalfonds is gratefully acknowledged.

REFERENCES

- ¹In order to avoid confusion with signs, the magnetic moment μ is taken positive: the spin vectors and the spontaneous magnetization, respectively, thus point along the *same* direction as the external magnetic field. This convention will be maintained throughout the paper.
- ²F.J. Dyson, Phys. Rev. **102**, 1217, 1230 (1956).
- ³S. Weinberg, Phys. Rev. Lett. **18**, 188, 507 (1967); Phys. Rev. **166**, 1568 (1968); R. Dashen, *ibid.* **183**, 1245 (1969); R. Dashen and M. Weinstein, *ibid.* **183**, 1261 (1969).
- ⁴S. Coleman, J. Wess and B. Zumino, Phys. Rev. **177**, 2239 (1969); C.G. Callan, S. Coleman, J. Wess and B. Zumino, *ibid.* **177**, 2247 (1969).
- ⁵L.-F. Li and H. Pagels, Phys. Rev. Lett. **26**, 1204 (1971); H. Pagels, Phys. Rep., Phys. Lett. **16C**, 219 (1975).
- ⁶S. Weinberg, Physica A **96**, 327 (1979).
- ⁷J. Gasser and H. Leutwyler, Ann. Phys. (N.Y.) **158**, 142 (1984); Nucl. Phys. B **250**, 465 (1985).
- ⁸P. Hasenfratz and H. Leutwyler, Nucl. Phys. B **343**, 241 (1990).
- ⁹P. Hasenfratz and F. Niedermayer, Phys. Lett. B **268**, 231 (1991).
- ¹⁰P. Hasenfratz and F. Niedermayer, Z. Phys. B **92**, 91 (1993).
- ¹¹J. Gasser and H. Leutwyler, Phys. Lett. B **184**, 83 (1987); *ibid.* **188**, 477 (1987).
- ¹²H. Leutwyler, Phys. Rev. D **49**, 3033 (1994); Helv. Phys. Acta **70**, 275 (1997).
- ¹³J.M. Roman and J. Soto, Int. J. Mod. Phys. B **13**, 755 (1999).
- ¹⁴J.M. Roman and J. Soto, Phys. Rev. B **62**, 3300 (2000).
- ¹⁵C.P. Hofmann, Phys. Rev. B **60**, 388 (1999).
- ¹⁶J.M. Roman and J. Soto, Ann. Phys. **273**, 37 (1999).
- ¹⁷C.P. Hofmann, Phys. Rev. B **60**, 406 (1999).
- ¹⁸C. P. Burgess and C. A. Lutken, Phys. Rev. B **57**, 8642 (1998).
- ¹⁹H. Leutwyler, in *Hadron Physics 94 – Topics on the Structure and Interaction of Hadronic Systems*, edited by V. E. Herscovitz, C. A. Z. Vasconcellos and E. Ferreira (World Scientific, Singapore, 1995), p. 1.; H. Leutwyler, hep-ph/0008124.
- ²⁰C.P. Burgess, Phys. Rept. **330**, 193 (2000).
- ²¹G. Ecker, hep-ph/9608226; Prog. Part. Nucl. Phys. **35**, 1 (1995); B.R. Holstein, hep-ph/0010033; hep-ph/9510344; V. Koch, Int. J. Mod. Phys. E **6**, 203 (1997); A.V. Manohar, in *Schladming 1996: Perturbative and Nonperturbative Aspects of Quantum Field Theory*, edited by H. Latal and W. Schweiger (Springer, 1997), p. 311; U.G. Meissner, Rept. Prog. Phys. **56**, 903 (1993); A. Pich, hep-ph/9806303.
- ²²C.P. Burgess, in *Radiative Corrections: Application of Quantum Field Theory to Phenomenology*, Barcelona, 1998, p. 471; hep-ph/9812468; G. Colangelo and G. Isidori, hep-ph/0101264; J. Gasser, Nucl. Phys., Proc. Suppl. **86**, 257 (2000); H. Leutwyler, hep-ph/9409422; L.F. Li, hep-ph/0001116.
- ²³We will only consider those terms in the higher order pieces of the effective Lagrangian which are relevant for the evaluation of the partition function. For a more general analysis the reader is referred to Ref.¹³.
- ²⁴The procedure is legitimate, since it merely corresponds to a change of variables.
- ²⁵We neglect contributions due to the anisotropy of the cubic lattice and assume space

rotation symmetry also at order p^4 and p^6 – the conclusions of the present work are not affected by this simplification.

- ²⁶ For a review of the effective Lagrangian method at nonzero temperature, see Refs.²⁷. For a general review of field theory at finite temperature, see Refs.²⁸.
- ²⁷ H. Leutwyler, Nucl. Phys. B, Proc. Suppl. **4**, 248 (1988); H. Leutwyler, in *Warsaw International Symposium on Elementary Particle Physics, Kazimierz, 1988 – New Theories in Physics*, edited by Z. Ajduk, S. Pokorski and A. Trautman (World Scientific, Singapore, 1989) p. 116; also in *Summer Institute in Theoretical Physics, Kingston, 1988 – Symmetry Violations in Subatomic Physics*, edited by B. Castel and P.J. O’Donnell (World Scientific, Singapore, 1989), p. 57.
- ²⁸ N.P. Landsman and C.G. van Weert, Phys. Rept. **145**, 141 (1987); J.I. Kapusta, *Finite Temperature Field Theory* (Cambridge University Press, Cambridge, 1989); A.V. Smilga, Phys. Rept. **291**, 1 (1997); J. Zinn-Justin, hep-ph/0005272.
- ²⁹ Note that we are now working in Euclidean space.
- ³⁰ R.D. Pisarski and M. Tytgat, hep-ph/9606459; hep-ph/9609414.
- ³¹ H.A. Kramers, Commun. Kamerlingh Onnes Lab. Univ. Leiden Suppl. **22**, 83 (1936); W. Opechowski, Physica **4**, 715 (1937).
- ³² M.R. Schafroth, Proc. Phys. Soc. London A **67**, 33 (1954).
- ³³ J. van Kranendonk, Physica **21**, 81, 749, 925 (1955).
- ³⁴ T. Morita, Prog. Theor. Phys. **20**, 614, 728 (1958); T. Oguchi, Phys. Rev. **117**, 117 (1960); F. Keffer and R. Loudon, J. Appl. Phys. (Suppl.) **32**, 2S (1961); D.C. Wallace, Phys. Rev. **153**, 547 (1967); V.G. Vaks, A.I. Larkin and S.A. Pikin, Sov. Phys. JETP **26**, 188 (1968).
- ³⁵ I. Mannari, Prog. Theor. Phys. **19**, 201 (1958); R. Brout and H. Haken, Bull. Am. Phys. Soc. **5**, 148 (1960); F. Englert, Phys. Rev. Lett. **5**, 102 (1960); R.A. Tahir-Kheli and D. ter Haar, Phys. Rev. **127**, 88, (1962); R.B. Stinchcombe, G. Horwitz, F. Englert and R. Brout, *ibid.* **130**, 155 (1963); H.B. Callen, *ibid.* **130**, 890 (1963); T. Oguchi and A. Honma, J. Appl. Phys. **34**, 1153 (1963).
- ³⁶ R.A. Tahir-Kheli and D. ter Haar, Phys. Rev. **127**, 95 (1962); I. Ortenburger, *ibid.* **136**, A 1374 (1964); T. Morita and T. Tanaka, *ibid.* **137**, A 648 (1965).
- ³⁷ P. Gerber and H. Leutwyler, Nucl. Phys. B **321**, 387 (1989).
- ³⁸ In fact, even the coefficient of the interaction term of order T^6 is fixed by the constant \mathcal{F} of the leading order Lagrangian \mathcal{L}_{eff}^2 – next-to-leading order couplings from \mathcal{L}_{eff}^4 only appear in a logarithmic scale T_Σ (see Refs.^{17,37}).
- ³⁹ C.P. Hofmann, unpublished.